Oxidation of organic matter in deep water: evidence for mediation of microbial weathering

Tasuku Akagi (akagi@geo.kyushu-u.ac.jp)
Kyushu University
Hirotaka Nishino
Kyushu University

Article

Keywords:

Posted Date: July 18th, 2022

DOI: https://doi.org/10.21203/rs.3.rs-1772754/v1

Abstract

Carbon fixed by phytoplankton in surface water is remineralized by oxidation, where a relationship among total inorganic carbon (TIC), dissolved inorganic phosphorus (DIP), nitrogen (DIN) and silicic acid is largely consistent with the Redfield ratio. In deep water, however, oceanic distribution of total inorganic carbon, TIC, does not reflect the Redfield ratio, but is correlated with silicic acid concentration over a wide geographical area, for a given concentration of DIN or DIP. Examination of existing datasets reveals that the relationship ΔTIC:Δalkalinity: ΔSi conforms to 1:~1:1.2 ~ 1.6 extensively. This C-Si stoichiometric relationship is difficult to understand in terms of conventional ideas based on the dissolution of carbonate and opal, in tandem with the oxidation of organic matter. This observation necessitates a re-evaluation of the cycling of oceanic Si and C. Here we propose that silicic acid in the deep ocean derives from weathering of silicate minerals, with aqueous CO_2 consumption balanced by the oxidation of organic carbon, perhaps microbially. In the deep ocean, aeolian dust – rather than fluvial input – is probably the major source of silicic acid. It is likely that the CO_2 balance between "CO_2 absorbing" dust weathering and "CO_2 releasing" organic carbon oxidation governs CO_2 exchange between the ocean and atmosphere. The C-Si stoichiometry collapses in upwelling areas of the North Pacific and Southern Oceans, resulting in the release of CO_2 from those regions.

Main Text

A proportion of the atmospheric carbon fixed by phytoplankton is transferred to the ocean depths, where it is degraded to particulate organic carbon and dissolved organic carbon (POC and DOC), then eventually oxidized to inorganic carbon. Carbon exchanges between the ocean and atmosphere in the form of CO_2. Therefore, the oxidation of organic carbon is an important process in controlling the storage of carbon in the ocean. Organic matter is oxidized by heterotrophic processes, which have, however, largely been unquestioned. Most fresh organic matter is readily oxidized in surface waters, with the proportion of refractory organic matter being increased in the deep water [1,2]. We consider how the organic matter in deep water is oxidized. Does it proceed in the same manner as in shallow water? To answer that question, we revisit the existing oceanic dataset.

The relationship between silicon concentration (as silicic acid) and TIC is shown in Fig. 1a [3]. TIC, dissolved inorganic nitrogen (DIN) and dissolved inorganic phosphorus (DIP) are usually strongly coupled in seawater (Fig. 1b), implying the same primary source of all three components (organic constituents of phytoplankton). The ratio carbon to nitrogen to phosphorus is a nearly constant 106:16:1 (the Redfield ratio) in dissolved nutrient pools (Fig. 1b, c). These components are remineralized on a similar timescale and are therefore subjected to the same advective flow, resulting in coherent behaviour [3]. However, closer inspection of Fig. 1a reveals that TIC depends only on silicic acid concentrations in the range 50 < [Si] < 150 μmol/kg. The contours of Fig. 1a denote nitrogen concentration. The straight contour lines indicate that TIC increases with [Si], for fixed [DIN]. In other words, both TIC and Si concentrations can increase independently of [DIN] (or [DIP], not shown) with ΔSi :ΔTIC typically 1.2 ~ 1.6. This is more evident in

Fig. 1c. Linear relationships between TIC and [DIP] (or [DIN], not shown), following the Redfield ratio, can be seen up to the maximum values of [DIN] or [DIP]. At high TIC values in Fig. 1c, however, additional TIC depending only on [Si] occurs at [Si] > 50 μmol/kg. This again shows the presence of a C and Si source, independent of N and P in the deep layer, where [Si] > 50 μmol/kg.

The TIC and alkalinity diagram shows TIC increase and alkalinity decrease largely with [DIP] (or [DIN], not shown) increase (Fig. 2b). This is primarily due to remineralization of planktonic organic matter, affected by carbonate formation and dissolution as indicated by the arrows in Fig. 2b. A similar feature is seen with [Si] in the region of [Si] < 50 μmol/kg, implying the supply of TIC and silicic acid due to planktonic degradation. However, alkalinity increase depends strongly on [Si] in the region of [Si] > 50 μmol/kg (Fig. 2a, inside oval). When there is a supply of carbon in the absence of P or N (Fig. 1), the slope (ΔTIC/Δalkalinity) passing through a certain [P] value (or [N] value, not shown) is ~ 1 or slightly lower (Fig. 2b). This alkalinity dependence on Si is not clear in the region of [Si] < 50 μmol/kg (Fig. 2a).

Here, we consider potential explanations for this simple but significant relationship of ΔTIC:Δalkalinity:ΔSi = 1:1:1.2 ~ 1.6.

Simple mixing of different water masses is in accord with the relationship shown in Fig. 1, if one end member has low [Si] and TIC whereas the other is characterized by high [Si] and TIC. However, [Si] in deep water is normally correlated with seawater density: isopycnic lines run almost vertically in Fig. 1a[3]. Therefore, the straight lines in Fig. 1a do not match isopycnic lines. The idea of mixing can thus be discounted.

This simple relationship of ΔTIC:Δalkalinity:ΔSi = 1:1:1.2 ~ 1.6 is achieved by carbonate dissolution, OC oxidation and opal dissolution at a molar ratio of 1:1:2.4 ~ 3.2. If this is a result of remineralization of settling particles, the ratio corresponds to $CaCO_3$:OM:opal weight ratio of 1:0.28: 1.5 ~ 2, assuming that OM is void of N and P. $CaCO_3$ dissolution and OM dissolution can be strongly coupled, as CO_2 produced by OM oxidation can be consumed in $CaCO_3$ dissolution. Also, OM is not limited to that in settling particles, but can be DOC. Therefore, OM contents in settling particles may not be restricted. The above $CaCO_3$:opal ratio of 1:1.5 ~ 2, however, poses three problems. Firstly, dissolution of $CaCO_3$ and opal take place independently: the former depends on carbonate saturation depth (CSD) and the latter mainly on water temperature. Close analysis reveals that the ΔTIC:Δalkalinity:ΔSi relationship at [DIP] = 2.5 μmol/kg (or [DIN] = 35 μmol/kg) includes data from depth shallower than CSD at [Si] = 50 ~ 60 μmol/kg, those from depth around CSD at [Si] = ~ 100 μmol/kg and those from depth deeper than CSD at [Si] = ~ 150 μmol/kg. This simply indicates that the three reactions (carbonate dissolution, OC oxidation and opal dissolution) cannot always be coupled with each other, but that carbonate dissolution reaction should decouple from the other two at areas of smaller [Si]. Secondly, opal export to deep water takes place in only a few regions, such as the North Pacific and the Southern Ocean[4]. When major dissolved Si input occurs only in North Pacific Deep Water (NPDW) and Antarctic Bottom Water (AABW), how can this input Si can be distributed to regions characterized by 50 < [Si] < 150 μmol/kg without resorting to mixing processes, which were discounted earlier? (Circulation of this input Si will be discussed later, in a different

context.) Thirdly, the $CaCO_3$:opal ratio in settling particles varies widely, by a factor up to 100[4]. If the Si is not sourced from NPDW or AABW, how could such a small variation in ΔTIC:Δalkalinity:ΔSi = 1:1:1.2 ~ 1.6 be attained over the wide range of 50 < [Si] < 150 μmol/kg?

A different explanation is that a 'weathering reaction' occurs in the ocean depths. Crustal material contains alkaline and alkaline-earth elements, dissolution of which generates not only silica, but also bicarbonate ion from oxide minerals. For example:

$$CaO + 2CO_2 + H_2O \rightarrow Ca^{2+} + 2HCO_3^- \quad (1)$$

$$Na_2O + 2CO_2 + H_2O \rightarrow 2Na^+ + 2HCO_3^- \quad (2)$$

If dust has the mineralogical composition typical of the upper crust [5], as expected, and contains 10% 'weathering-resistant' quartz[6], the ratio of total HCO_3^- to Si (ΔHCO_3^- /ΔSi) produced by dissolution will be ~ 0.7, i.e. almost identical to the slope observed in Fig. 1a. However, CO_2 should be replenished, in order to maintain ΔTIC/ΔSi ~ 0.7. In principle, this may be achieved by the parallel oxidation of organic carbon (OC). If this is indeed the case, the combined reactions yield TIC, alkalinity and Si at a ratio of 1:1:1.4. The slightly lower than unity TIC:alkalinity ratio in Fig. 2b could be the result of secondary carbonate formation/dissolution reactions. The layer of [P] around 3 μmol/kg in the Pacific Ocean corresponds to the depth where carbonate formation is supposed to occur.

It has been reported that the weathering reaction can be mediated by microorganisms in marine environments [7,8]. Therefore, it is reasonable to consider that those organisms harness energy by oxidizing OC and that they obtain micronutrients (such as Fe) by dissolving silicate minerals. This mechanism can generate silicic acid and HCO_3^- simultaneously, thus explaining the alkalinity increase being dependent on [Si] increase (Fig. 2a). Interestingly, the vertical distribution of dissolved organic carbon (DOC) and particulate organic carbon (POC) is the mirror image of that of [Si]. Furthermore, the magnitude of [Si] increase is similar to that of DOC decrease[9]. Although this combination of dust weathering and OC oxidation has not been proposed previously, it does provide a potential interpretation of the relationship shown in Figs. 1 and 2.

Based on the above discussion, there are two different combinations of remineralized materials which could form the basis of a possible explanation: (1) carbonate, OC and opal; alternatively (2) dust and OC. We now further examine the possibility of novel combination 2.

The spatial variation of K/Na or Mg/Na in seawater with changes of silicic acid concentration might provide further support of the proposed weathering. If a silicic acid concentration change of 100 μmol/kg is the result of dust weathering, calculation predicts 0.02% and 0.1% increase in Mg/Na and K/Na, respectively. However, the precision of measurements is not high enough to detect such differences[10].

Weathering of silicate dust in an aqueous phase produces HCO_3^-, with p_{CO2} of the water being depleted unless CO_2 is replenished by the oxidation of OC. Therefore, when the silicic acid concentration increases without an increase in TIC, the aqueous phase becomes alkaline and depleted in CO_2. Alternatively, if OC oxidation occurs without silicate dust weathering, p_{CO2} of the aqueous phase will increase and the phase becomes more acidic. A test of whether the process of silicate dust weathering to release silicic acid operates in the deep ocean is to compare the chemical composition of the seawater with the propensity of the seawater to release or absorb CO_2.

We first express TIC as a function of [Si] and [DIN] by analyzing data from depths greater than 500 m to avoid the surface mixing layer, which shows a 'noisy' relationship between TIC, [Si] and [DIN]. The slope of $\Delta TIC/\Delta Si$ tends to decrease from 0.8 to 0.4 with increasing [Si]. As the most important layer is the uppermost depth of 500 m, where [Si] is largely < 60 μmol/kg, data with [Si] < 60 μmol/kg was used. The reason for the decreasing slope with increasing [Si] will be considered in relation to upwelling water, towards the end of this paper. The function obtained is:

$$[TIC] = 2194 + 0.8\,[Si] + 7.56([N] - 32.1). \quad (3)$$

The water that satisfies this equation is assumed to be well balanced between "CO_2 absorbing" dust weathering and "CO_2 releasing" organic carbon remineralization. We then introduce an index B_{OW}, denoting deviation of [TIC] from the balance associated with "ocean weathering", to evaluate whether CO_2 would be absorbed or released during water circulation.

$$B_{OW} = [TIC] - 7.56([N] - 32.1) - 0.8[Si] - 2194 \quad (4)$$

If the B_{OW}-index is negative, it is likely that the p_{CO2} is not yet recharged from OC decay. This water is likely to absorb CO_2 when it rises towards the surface. On the other hand, if the B_{OW}-index is positive, OC degradation exceeds the weathering effect. This water should release CO_2, when it flows towards the surface.

The second possibility, namely of dust and OC coupling, if true, may be seen in the present-day oceans. Surprisingly excellent matches of the B_{OW}-index values with surface p_{CO2} are seen (Fig. 3a, d): the CO_2-releasing east central Pacific Ocean shows positive B_{OW}-index values. Furthermore, that locality's Sub-tropical Mode Water forms, which are well-known to be CO_2-absorbing, exhibit negative B_{OW}-index values. In reality, the uppermost depth (500m), where B_{OW}-index values can be calculated, is overlaid by the surface mixed layer. The tendency of water to release or absorb CO_2 may be disguised (at least partially) by the presence of this layer and also by carbonate buffering of p_{CO2}. Existing models of surface p_{CO2} require a supply of Fe from dust [11]. Furthermore, a dependence on surface water temperature is also needed to reproduce the observed surface p_{CO2} [11]. It should be noted that neither Fe abundance nor water temperature are considered in the B_{OW}-index we present here. If carbonate and opal dissolution + OC

oxidation (combination 1) are operative, excess Si or TIC excess should not relate directly to whether CO_2 is retained in the ocean water or is released to the atmosphere.

It should be noted that, as our B_{OW}-index is defined using data for water deeper than 500 m, it is pointless to show its value for surface waters. In addition, the above discussion implies that the surface-layer water merely equilibrates with the atmosphere with respect to CO_2 and is therefore of little importance in regulating atmospheric p_{CO2}. This is consistent with the observation that surface production plays little role in carbon transport to the ocean interior [12].

If we accept the importance of airborne dust input to the sea surface (as an alternative to riverine sources), the oceanic silicon budget may be greatly affected. If the Si responsible for $\Delta TIC/\Delta Si = 0.7$ is ultimately derived from dust, this would account for about half of the silicate supplied to the oceans, on a global scale. The contribution of airborne dust is comparable to that of riverine silicic acid, thus probably the residence time of silicon may be smaller than has been estimated previously [13]. We suggest that investigating for the presence of surficial bacteria on dust particles associated with weathering would be helpful here.

The proposed weathering process in the oceans implies that carbon can be retained in the oceans as inorganic carbon, coupled with the accumulation of silicic acid in a 'normal' deep ocean, where $50 < [Si] < 150$ μmol/kg (Fig. 4a). Close comparison between the B_{OW}-index and the observed p_{CO2} distribution reveals a discrepancy between them in the North Pacific: the B_{OW}-index shows negative values (Fig. 3a), but the observed p_{CO2} indicates emission from the same area (Fig. 3d).

The North Pacific is an active area of upwelling and diatom production is high. We have postulated "dissolution kinetics of diatom aggregates" to explain the chemical composition of diatom frustules[14,15] and to reproduce the opal distribution, which is consistent with the observed Al distribution[16]. Based on this kinetic explanation, frustules form larger aggregates in regions of high diatom productivity and a greater portion of opal dissolves in deeper waters. Owing to rapid remineralization, carbon tends to remain as CO_2 in the surface water, whereas in upwelling areas more frustules escape dissolution. In such upwelling areas, carbon abundance is therefore decoupled from [Si], resulting in collapse of the stoichiometric relationship between TIC and Si. In the surface water of such areas, accumulated CO_2 has to be removed to the atmosphere to meet a steady state, while Si is selectively exported to the deep water. In deep water of such areas, $\Delta TIC/\Delta Si$ decreases to almost zero, as can be seen in Fig. 1a; this implies loss of carbon from those regions (Fig. 4b). This is able to explain the discrepancy seen in the comparison of the B_{OW}-index and p_{CO2} values in the North Pacific (Fig. 3a, d). It is interesting to note that, in Fig. 1a, the Southern Ocean – another upwelling-active area – also displays a clear departure from the linear relationship. The East Central Pacific ocean is also known as an upwelling dominant area [17]. Unfortunately, stations of our dataset are not exactly on the equator. The B_{OW} index already shows the feature of CO_2 releasing, which is likely to be further boosted by upwelling. This is the reason why this area is known as the most active CO_2 releasing zone. The zero $\Delta TIC/\Delta Si$ can also be explained by the

dissolution of silicic acid from the seafloor [18]. This may occur, but water showing ΔTIC/ΔSi = 0 includes intermediate water [3] and it is considered that the loss of CO_2, coupled with efficient export of Si from the surface layer, is the main reason for the zero ΔTIC/ΔSi. If some opal deposition from the water column onto the seafloor occurs, this should also contribute to the collapse of the stoichiometry or deviation from the linear relationship.

The CO_2 flux from upwelling areas can be estimated from the corresponding deviation (Fig. 4c), mass flow data of upwelling, and opal burial rates in those areas[18]. In the North Pacific, estimation of the mass transport is complicated [19]. For the Southern Ocean, however, using mass transport data for upwelling [20], CO_2 emission is calculated (as the product of mass transport rate and the extent of deviation from linearity) to be around 30 Tmol/year. The contribution of opal burial is not included in this calculation, but it is less than 10%. This estimate is very small compared to the rate of total carbon exchange between the ocean and atmosphere, but is comparable to the carbon removal rate attributed to terrestrial weathering [21]. Nevertheless, this CO_2 emission could be crucial to the oceanic carbon budget, as it is not readily 'cancelled out' because of originating from the deep ocean. It can therefore be a critical component for understanding carbon budget variations during the transition between glacial and interglacial stages. It is widely accepted that a proportion of the carbon sequestered by the ocean during glacial times was returned to the atmosphere during deglacial times[22]. Such a mechanism explains very well that CO_2 is released during deglacial times, in tandem with an increase in opal burial [23].

Incidentally, it has been argued that the 'unexploited' high abundance of DIN in the Southern Ocean, together with Si depletion, are exported to (and affects the biological productivity of) lower latitudes by sub-Antarctic mode water (SAMW) of typical density (σ_θ) = 26.8 [24]. However, as shown in Fig. 3c, it is clear that B_{OW} does not propagate during the transportation. The tendency of water to absorb/release CO_2 should be acquired rather locally by the addition of dust or oxidation of OC.

The mechanism developed in this paper does not contradict observations of opal flux in the oceans4. Significantly, high opal export is only seen in upwelling-active areas, where the (ΔTIC/ΔSi) stoichiometric relationship has collapsed. In many regions, where the observed (ΔTIC/ΔSi) ratio of ~ 0.6 to 0.8 applies, opal export to deep water is smaller than 30 mmolSi $m^{-2}yr^{-1}$ (ref. 4). This is consistent with Si increasing by 10 μmol/kg or less in the deep water, during the time taken to flow from the North Atlantic to the North Pacific (~ 1000 year). However, such an increase is significantly smaller than as shown by observations.

Deep water to which silica is added in the upwelling areas (see Fig. 4) eventually flows elsewhere, transported by Pacific Deep Water (PDW) in the Pacific or by Antarctic Bottom Water (AABW) in the Atlantic. This is clearly evident in the B_{OW} -index values at 2000 m depth (Fig. 3b), which are more uniform and closer to zero than those at 500 m depth (Fig. 3a). This indicates that the deep water is almost in balance, with respect to CO_2. Nevertheless, because of the 'excess' Si supplied from deep water in the upwelling areas, the B_{OW}-index values are negative in the North Pacific and in the Southern Ocean. This may appear as a depression in the slope of ΔTIC/ΔSi seen in Fig. 1a and may explain why ΔTIC/ΔSi

in Fig. 1a decreases with the increase of silicic acid concentration. Selecting datasets in which [Si] < 60 µmol/kg ensures that there is balance between "CO_2 absorbing" dust weathering and "CO_2 releasing" organic carbon remineralization, as expressed by Eq. 3. For [Si] < 60 µmol/kg, significant deviation in the (ΔTIC/ΔSi) ratio due to influence of "upwelling active areas" is avoided.

This study is supported by Grant-in-Aid from MEXT (No. 17K05717).

Declaration

Data availability

The datasets analysed during the current study are available in the "*eWOCE - Electronic Atlas of WOCE Data*" repository, https://www.ewoce.org/data/index.html#WHP_Bottle_Data

References

1. Druffel, E. R., Williams, P. M., Bauer, J. E. & Ertel, J. R. Cycling of dissolved and particulate organic matter in the open ocean. Journal of Geophysical Research: Oceans **97**, 15639–15659 (1992).
2. Raymond, P. A. & Bauer, J. E. Riverine export of aged terrestrial organic matter to the North Atlantic Ocean. Nature **409**, 497–500 (2001).
3. WOCE Data Products Committee, 2002. Available from: http://www.ewoce.org/.
4. Honjo, S., Manganini, S. J., Krishfield, R. A. & Francois, R. Particulate organic carbon fluxes to the ocean interior and factors controlling the biological pump: A synthesis of global sediment trap programs since 1983. Progress in Oceanography **76**, 217–285, doi:10.1016/j.pocean.2007.11.003 (2008).
5. Rudnick, R. & Gao, S. Composition of the continental crust. Treatise on geochemistry **3**, 1–64 (2003).
6. Ronov, A. & Yaroshevsky, A. Chemical composition of the earth's crust. The Earth's crust and upper mantle **13**, 37–57 (1969).
7. Vorhies, J. S. & Gaines, R. R. Microbial dissolution of clay minerals as a source of iron and silica in marine sediments. Nature Geoscience **2**, 221–225 (2009).
8. Cozzi, S., Ivančić, I., Catalano, G., Djakovac, T. & Degobbis, D. Dynamics of the oceanographic properties during mucilage appearance in the Northern Adriatic Sea: analysis of the 1997 event in comparison to earlier events. Journal of Marine Systems **50**, 223–241 (2004).
9. Pakulski, J. D. & Benner, R. Abundance and distribution of carbohydrates in the ocean. Limnology and Oceanography **39**, 930–940 (1994).
10. Riley, J. & Tongudai, M. The major cation/chlorinity ratios in sea water. Chemical Geology **2**, 263–269 (1967).
11. Tjiputra, J. F. *et al.* Long-term surface pCO2 trends from observations and models. Tellus B: Chemical and Physical Meteorology **66**, 23083 (2014).

12. Francois, R., Honjo, S., Krishfield, R. & Manganini, S. Factors controlling the flux of organic carbon to the bathypelagic zone of the ocean. Global Biogeochemical Cycles **16**, 34-31-34–20 (2002).
13. Treguer, P. *et al.* The silica balance in the world ocean: a reestimate. Science **268**, 375–379, doi:10.1126/science.268.5209.375 (1995).
14. Akagi, T., Fu, F.-f., Hongo, Y. & Takahashi, K. Composition of rare earth elements in settling particles collected in the highly productive North Pacific Ocean and Bering Sea: Implications for siliceous-matter dissolution kinetics and formation of two REE-enriched phases. Geochimica et Cosmochimica Acta **75**, 4857–4876, doi:http://dx.doi.org/10.1016/j.gca.2011.06.001 (2011).
15. Akagi, T. Revision of the dissolution kinetics of aggregated settling particles. Mem. Fac. Sci. Kyushu Univ. Ser. D Earth & Planet. Sci. **33**, 1–5 (2013).
16. Akagi, T. & Nishino, H. Unified modeling of contrasting basin-scale dissolved Al distributions using dissolution kinetics of diatom aggregates: Implication for upwelling intensity as a primary factor to control opal burial rate. Marine Chemistry **235**, 104009 (2021).
17. Fiedler, P. C., Philbrick, V. & Chavez, F. P. Oceanic upwelling and productivity in the eastern tropical Pacific. Limnology and oceanography **36**, 1834–1850 (1991).
18. Tréguer, P. J. & De La Rocha, C. L. The world ocean silica cycle. Annual review of marine science **5**, 477–501 (2013).
19. You, Y. *et al.* Transport of North Pacific intermediate water across Japanese WOCE sections. Journal of Geophysical Research: Oceans **108** (2003).
20. Talley, L. D. Closure of the global overturning circulation through the Indian, Pacific, and Southern Oceans: Schematics and transports. Oceanography **26**, 80–97 (2013).
21. Houghton, R. A. The contemporary carbon cycle. Treatise on geochemistry **8**, 473–513 (2003).
22. Sigman, D. M. & Boyle, E. A. Glacial/interglacial variations in atmospheric carbon dioxide. Nature **407**, 859–869, doi:Doi 10.1038/35038000 (2000).
23. Anderson, R. *et al.* Wind-driven upwelling in the Southern Ocean and the deglacial rise in atmospheric CO2. *science* **323**, 1443–1448 (2009).
24. Sarmiento, J. L., Gruber, N., Brzezinski, M. & Dunne, J. High-latitude controls of thermocline nutrients and low latitude biological productivity. Nature **427**, 56–60 (2004).

Figures

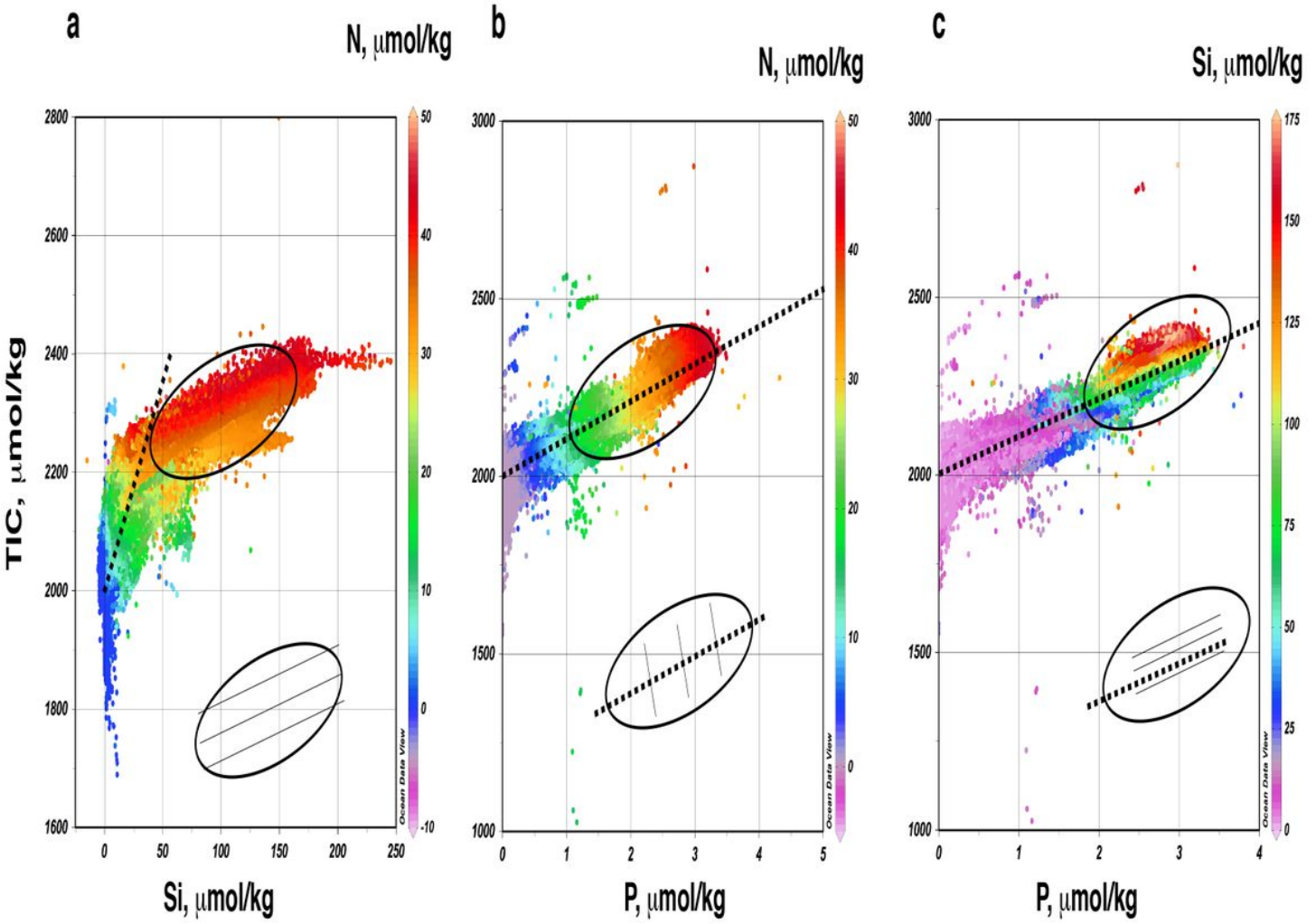

Figure 1. Akagi and Nishino

Figure 1

(a). The relationship between TIC and silicic acid. Colours indicate the associated concentrations of DIN. Parallel gradation can be seen in the range 50 < [Si] <150 µmol/kg, with slope smaller than the Redfield ratio (black broken line).

(b). The equivalent relationship between TIC and DIP. Here, the colours indicate [DIN], with gradations being almost perpendicular to the Redfield line.

(c). As for (b), but colours denote [Si]. Note that contours run parallel to the Redfield line.

The relationships illustrated in (a), (b) and (c) are shown schematically in the lower ovals. Data are from ref. (2) and processed with Ocean Data View.

The relationship illustrated in (a) to (c) indicate the presence of silicon and carbon sources (not supplying DIN and DIP) in deep water with [Si] > 50 μmol/kg.

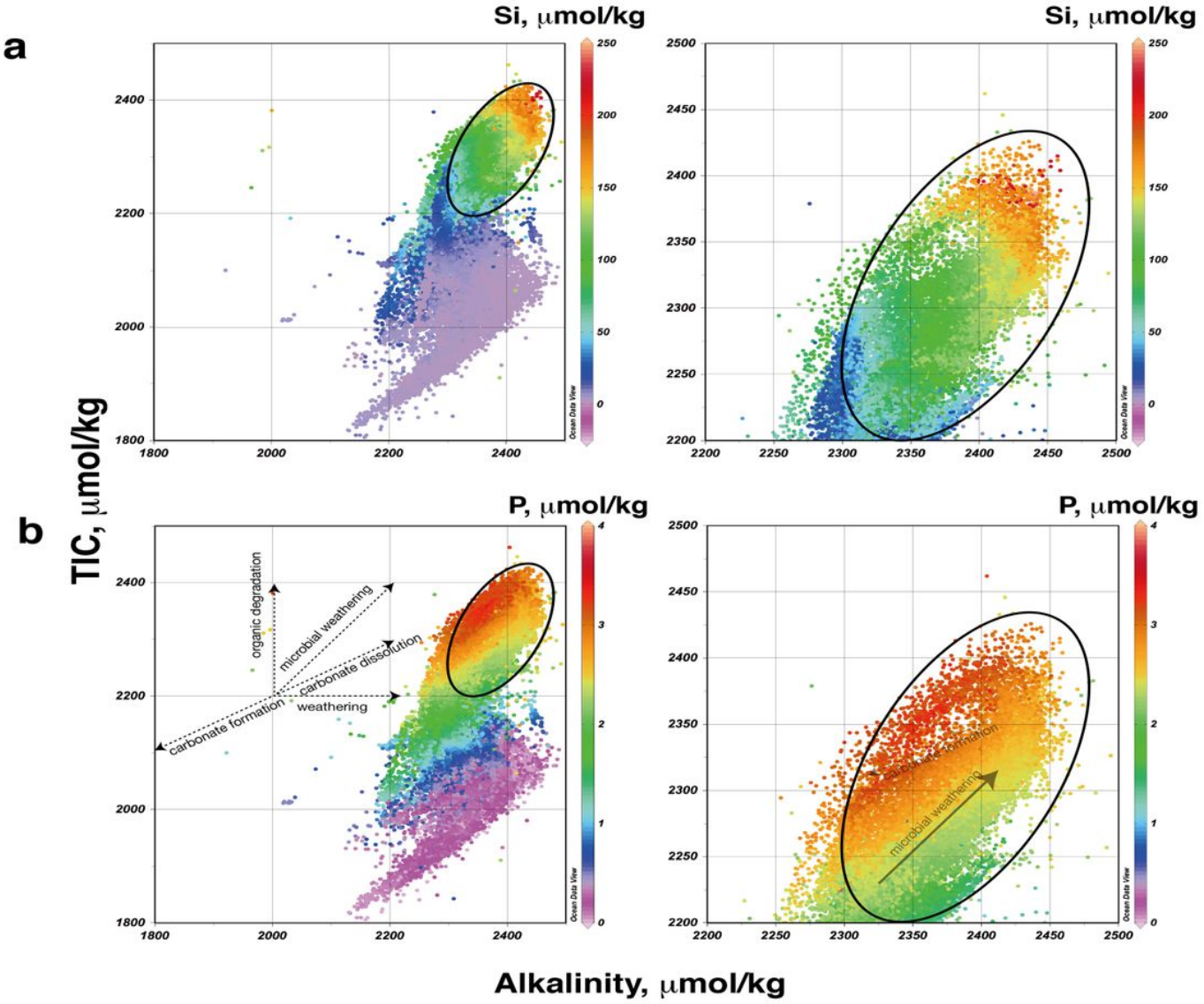

Figure 2. Akagi and Nishino

Figure 2

Alkalinity and TIC relationship. Colours indicate [Si] in (a) and [DIP] in (b). The two plots on the right are enlarged version of the respective adjacent plots. Ovals indicate data corresponding to [Si] > 50 μmol/kg. Vectors of the relevant reactions are shown on the Alkalinity-TIC plane.

In the deep water of [Si] > 50 μmol/kg (region in the oval), alkalinity increases with [Si] increase (a). A contour through a fixed [DIP] value gives a linear slope, which corresponds to that of microbial weathering (b). Taking into account that the carbon change at a constant [DIN] and [DIP] is coupled with [Si] change in this water (Fig. 1), Δ[Si]:ΔTIC:Dalkalinity is identical to that of microbial weathering.

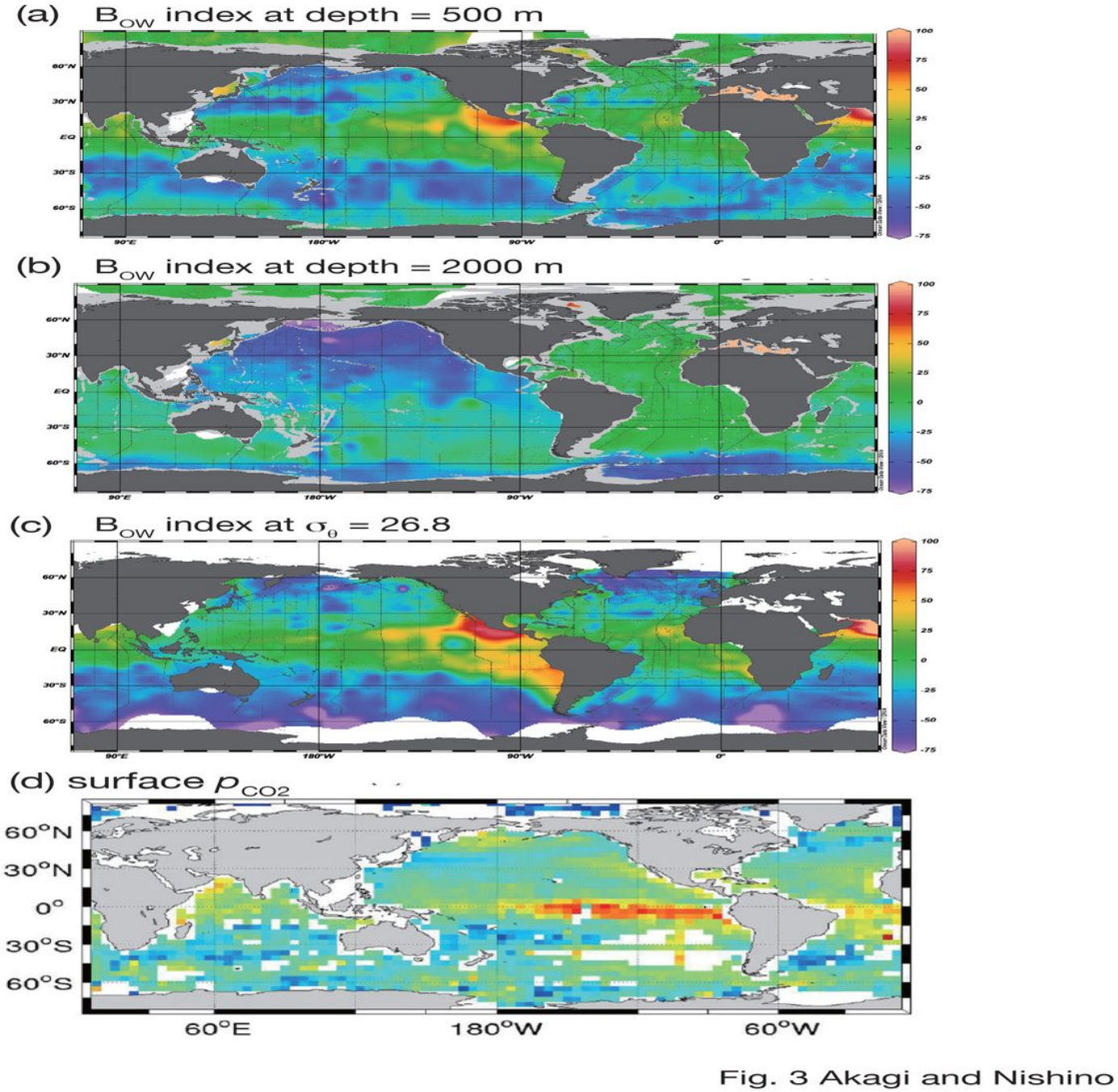

Fig. 3 Akagi and Nishino

Figure 3

B_{OW}-index values at depths of 500 m and 2000 m are shown (a) and (b) respectively. B_{OW}-index values at density σ_θ = 26.8 are shown in (c). In contrast, (d) shows the observed p_{CO2} distribution in surface water.

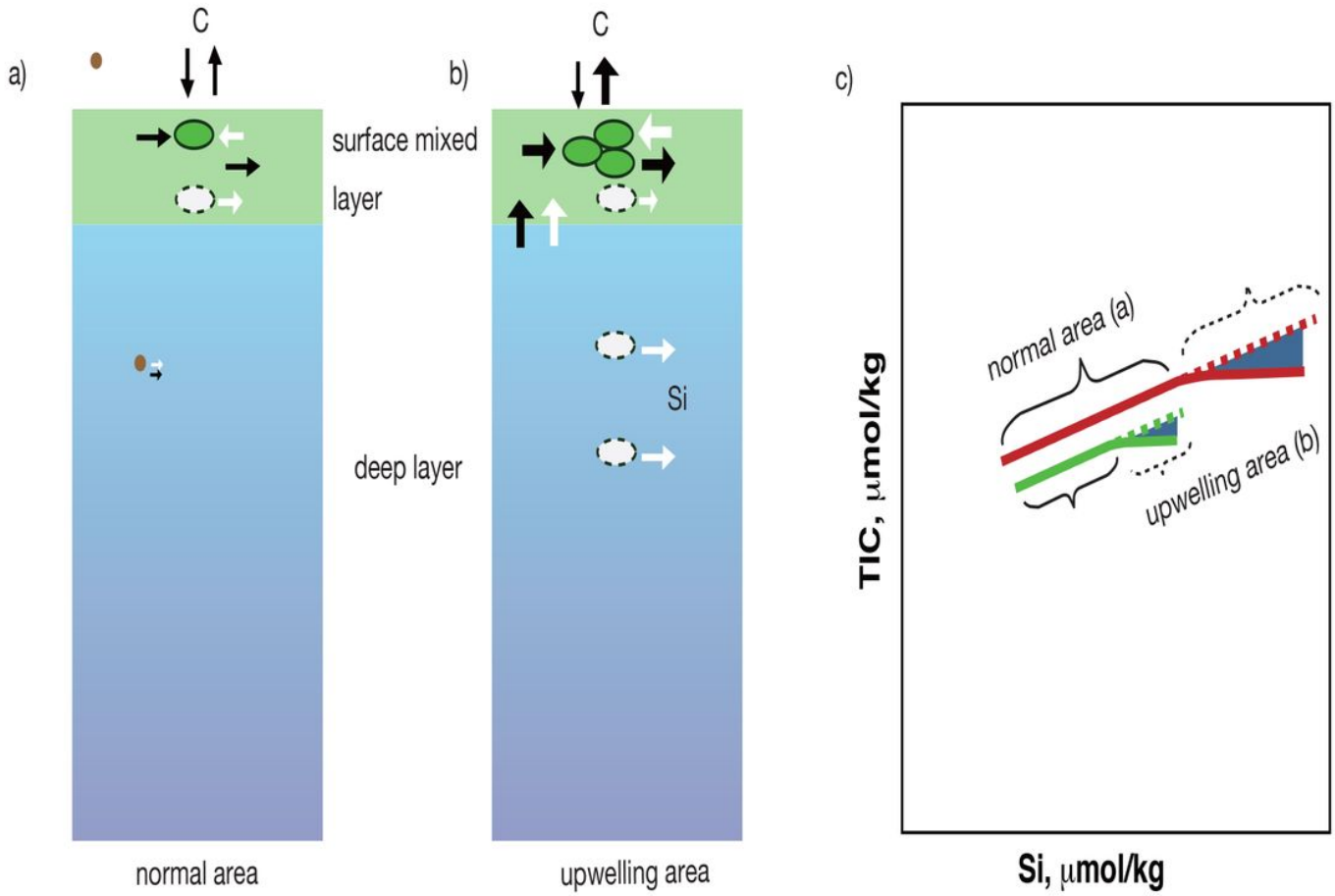

Fig. 4 Akagi & Nishino

Figure 4

Comparison of oceanic carbon and silicon budgets in a 'typical' (non-upwelling) area (a) and an upwelling area (b), as represented by the relationship between [Si] and TIC in the Pacific Ocean (red) and Southern Ocean (green). Black and white arrows represent flows of carbon and silicon, respectively. Ovals indicate diatoms, whereas the brown dot represents dust. In (c), discrepancies between solid and broken lines (shadowed area) in upwelling regions correspond to carbon released to the atmosphere, neglecting any contribution attributable to opal deposition. If opal deposition is taken into account, more carbon should be released to the atmosphere.